machines

MDPI

Article

Effect of Wiper Edge Geometry on Machining Performance While Turning AISI 1045 Steel in Dry Conditions Using the VIKOR-ML Approach

Adel T. Abbas [1,*], Neeraj Sharma [2], Mahmoud S. Soliman [1], Magdy M. El Rayes [1], Rakesh Chandmal Sharma [3] and Ahmed Elkaseer [4]

[1] Department of Mechanical Engineering, College of Engineering, King Saud University, P.O. Box 800, Riyadh 11421, Saudi Arabia
[2] Department of Mechanical Engineering, Maharishi Markandeshwar Engineering College, Maharishi Markandeshwar (Deemed to be University), Mullana 133207, India
[3] Department of Mechanical Engineering, Graphic Era (Deemed to be University), Dehradun 248002, India
[4] Institute for Automation and Applied Informatics, Karlsruhe Institute of Technology, 76344 Eggenstein-Leopoldshafen, Germany
* Correspondence: aabbas@ksu.edu.sa

Abstract: AISI 1045 can be machined well in all machining operations, namely drilling, milling, turning, broaching and grinding. It has many applications, such as crankshafts, rollers, spindles, shafts, and gears. Wiper geometry has a great influence on cutting forces (F_r, F_f, F_c and R), temperature, material removal rate (MRR) and surface roughness (R_a). Wiper inserts are used to achieve good surface quality and avoid the need to buy a grinding machine. In this paper, an optimization-based investigation into previously reported results for Taguchi's based L_{27} orthogonal array experimentations was conducted to further examine effect of the edge geometry on the turning performance of AISI 1045 steel in dry conditions. Three input parameters used in current research include the cutting speed (V_c), feed (f) and depth of cut (a_p), while performance measures in this research were R_a, F_r, F_f, F_c, R, temperature (temp) and MRR. The Vise Kriterijumska Optimizacija Kompromisno Resenje (VIKOR) method was used to normalize and convert all the performance measures to a single response known as the VIKOR-based performance index (V_i). The machine learning (ML) approach was used for the prediction and optimization of the input variables. A correlation plot is developed between the input variable and V_i using the ML approach. The optimized setting suggested by V_i-ML is V_c: 160 m/min; a_p: 1 mm and f: 0.135 mm/rev, and the corresponding value of V_i was 0.2883, while the predicted values of R_a, F_r, F_f, F_c, R, temp and MRR were 2.111 µm, 43.85 N, 159.33 N, 288.13 N, 332,16 N, 554.4 °C and 21,600 mm^3/min, respectively.

Keywords: cutting forces; machine learning; R_a; VIKOR; wiper insert

Citation: Abbas, A.T.; Sharma, N.; Soliman, M.S.; El Rayes, M.M.; Sharma, R.C.; Elkaseer, A. Effect of Wiper Edge Geometry on Machining Performance While Turning AISI 1045 Steel in Dry Conditions Using the VIKOR-ML Approach. *Machines* **2023**, *11*, 719. https://doi.org/10.3390/machines11070719

Academic Editor: Qingshun Bai

Received: 10 June 2023
Revised: 26 June 2023
Accepted: 4 July 2023
Published: 6 July 2023

1. Introduction

The 1045 steel alloys are very common in the manufacturing sector and have many applications, such as connecting rods, a crankshaft, gears, bolts, shafts, etc. The machining techniques to process AISI 1045 steel alloys were fully developed, but to obtain higher productivity and good surface quality, researchers are still working in this direction. The research community is working on the development of advanced techniques in machining and optimization by which better productivity and surface quality can be obtained.

Nowadays, controlling surface quality along with productivity is the requirement of most of these industries and is the most difficult challenge for researchers. In the manufacturing process, the raw material was converted into the finished products so as to be used for different applications. Therefore, an item with enhanced features and being financially stable are important aspects to be taken into consideration [1,2]. Almost 95%

of the energy during machining is transformed into heat due to the movement between the workpiece and the tool to be machined [3,4]. The energy formed is waste, and surface quality, along with tool, wear also suffers [5]. Although fast machining is preferable in order to have excellent productivity, the cutting speed is restricted because of the relative motion of the tool and the workpiece. Therefore, it is better to control the heat generated in order to have a good quality product and also an improved tool life. Additionally, such heat causes the microstructural distortion of the components [6]. The quality of these components is also compromised due to the relative motion between the material and the tool [7]. This issue can be solved by introducing the cutting fluids on the interface of the tool and workpiece [3,8]. The prime utilization of such fluids is to overcome the heat produced at the interface of the tool and workpiece [9]. Other than this, it also overcomes the friction between the tool and material during the machining [10]. Additionally, cutting fluids help to remove the metal chips during machining [11], and coolants make the tool–work interface chips free and ensure smoothness over the workpiece [12]. These features of coolants and lubricants enable their utilization in various procedures such as drilling, grinding, turning, etc. [13]. The mechanism of deformation is greatly impacted by the cooling technique that is applied [14]. Although coolants and lubricants have a number of benefits, they also have certain outcomes as well [12]. During machining, the usage of coolants and lubricants facilitates the colonization of fungi and bacteria [15]. Not only this, coolants and lubricants are made up of cryogenic materials [16], which can cause an allergy or cancer when it comes in contact with the skin of humans [17]. Additionally, they enhanced the manufacturing expenses by 8% of the total expenses, which is important when taken into consideration for a daily scenario [18]. Therefore, to overcome the drawbacks of coolants and lubricants, various investigators have focused on finding alternatives to coolants and lubricants while considering the advantages of the two. NDM (Near dry machining) is a stride toward using fewer coolants and lubricants while machining [12]. The main purpose of NDM is to ensure green and sustainable manufacturing in the latest environment [19–23]. NDM is exceptionally advantageous for greener and more sustainable processes [24]. Taguchi defines the item's nature as "the base loss is ensured whenever the item [is] dispatched among the general public" [25]. The overall loss is considered a combination of spending by the clients, disappointment, a guarantee of cost, loss because of a network, the mismanagement of assets, and so on. One of the methodologies is robust design in order to find the circumstances of the process and product, which can ensure low expenses in production and good quality products. One such technique is the Taguchi approach, which ensures the optimization of quality, cost and performance. The most important tools for robust design are the signal-to-noise ratio and orthogonal arrays. The former ensures good quality for the outcomes and later contains various control factors. Taguchi's technique completely supports the trials of the measurable plan. This approach fulfills the advancement in the process and reduces the time needed for the experimental examination [26–28]. Various practitioners and researchers have used the DOE (design of experiments) and its upgradation to Taguchi's method to make a strategy for the experiments and also perform the optimization of the parameters for machining. In Bajić et al. [29], a sequence of experimentation was carried out with DOE so as to examine how surface roughness became impacted by the cutting parameters such as a_p, f and V_c in the operation of face milling. Yang and Chen [30] used the Taguchi method to plan the process, which eventually ensured an exact technique that could productively differentiate the perfect surface roughness. In Filho and Diniz [31], DOE was utilized in order to examine the effect of surface finish, tool wear, the feed rate per tooth, and cutting velocity in contrast with the processing activity. Tsao [32] projected another technique named Gray–Taguchi in order to improvise the parameters for the aluminum combination, which demonstrated good finishing over the surface. The literature states how various investigators have studied machining in the field of the DOE and NDM application. However, some issues have arisen while considering the NDM idea, which signifies that more research must be carried out so as to find out a reasonable panacea.

After the review of the literature, it was found that numerous research has been conducted on the processing of steel by a carbide tool [33–35]. Another aspect of research by investigators is using the one parameter at a time approach, the Taguchi method and the Grey relational approach. However, a dearth of research has reported on the processing of AISI 1045 steel using the wiper geometry tool insert [36]. However, few works of research have been published on the implementation of the VIKOR-ML approach to investigate performance measures while processing AISI 1045 steel using wiper tool inserts. The planning of this experiment is conducted using the Taguchi-based L_{27} orthogonal array. The V_c, f and a_p were the input variables, while R_a, F_r, F_f, F_c, R, temp and MRR were the performance measures. All the output variables were changed into a single performance measure, termed the performance index, and this was investigated using VIKOR. Thus, this is known as the VIKOR-based performance index (V_i). The machine learning approach was used for the investigation and correlation of the V_i with the input variables.

2. Materials and Methods

This manuscript presents an extended investigation into the machining responses of AISI 1045 steel under dry turning conditions, previously reported by Abbas et al. [35,36]. The material processed in the present work was AISI 1045 steel. This steel has applications in different industries, requiring high strength and wear resistance. Table 1 provide the composition (chemical) and mechanical characteristics of the material.

Table 1. Compositions (Chemical) and mechanical characteristics for AISI 1045 [35].

Element	S	P	Mn	C	Fe
Percentage %	0.04	0.03	0.65	0.45	Balance
Characteristics				Value	
Hardness, Vickers				170	
Young's Elasticity				200 GPa	
Reduction in Area				40%	
Tensile Strength, Yield				310 MPa	
Tensile Strength, Ultimate				565 MPa	
Elongation at Break (in 50 mm)				16%	

The bars of AISI 1045 steel were received in hot-rolled and normalized conditions. For microstructural testing, the steel bars were sawed into small samples using a coolant in order to avoid excessive heating. For metallographic preparation, the steel samples were ground using SiC sandpaper with different grit sizes, after which polishing was performed using a polishing cloth and colloidal silica suspension. This was followed by an etching process using 2% Nital solution for 10 s which was subsequently washed and dried. This was followed by an etching process using a 2% Nital solution for 10–20 s which was subsequently washed and dried. The microstructure was examined using the scanning electron microscope, SEM (JEOL-6600, Tokyo, Japan). Figure 1a shows a secondary electron image (SEI) on the etched surface. The microstructure was composed of fine grains of proeutectoid α-ferrite (dark phase) and fine pearlite (lamellar structure of ferrite (dark phase) and cementite, Fe_3C, white phase). The microstructure represents a typical example of normalized hypoeutectoid plain carbon steel.

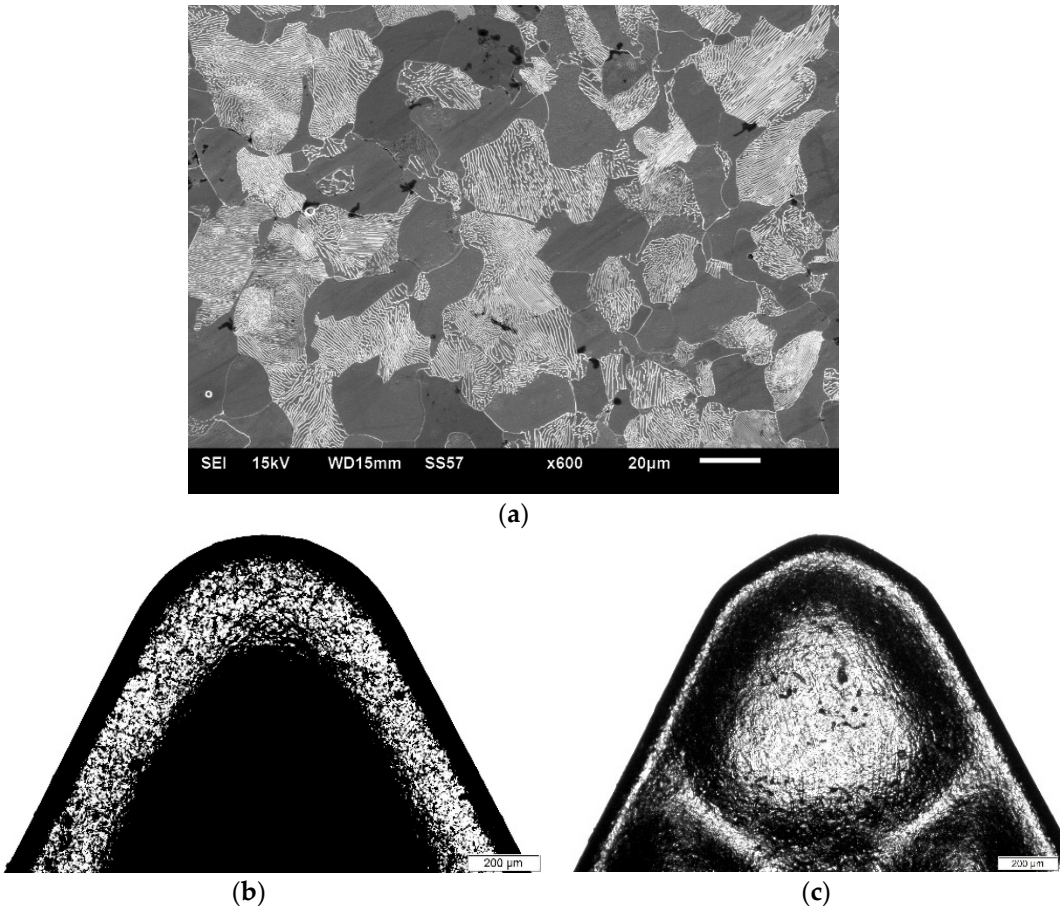

(**a**)

(**b**) (**c**)

Figure 1. (**a**) Microstructure of AISI 1045 steel; Microscopic image of (**b**) Normal (**c**) Wiper geometry Carbide Tool inserts [36].

The conventional lather of the Emco make (EMCOMAT-20D, Hallein-Taxach, Austria) was used to machine the material [37]. This machine tool had the following specifications: Electronic speed control: 40–3000 rpm, longitudinal feed: 0.045–0.787 mm/rev, drive motor: 5.3 kw and stepless speeds. The Sandvik make (Stockholm, Sweden) carbide tool insert with wiper geometry (DCMX11 T304-WF 4315) was used to process AISI 1045 steel with a length of 120 mm, diameter of 70 mm and cutting length of 30 mm for each pass was used for the experimentation [35,36].

A total of 27 test runs were as follows: three levels of surface speed (V_c) 80, 120, and 160 m/min, three levels of depth of cut (a_p): 0.5, 0.75, and 1.0 mm, three levels of the feed rate (f): 0.045, 0.09, and 0.135 mm/revolution [35,36]. Figure 2 depicts the microscopic image of a normal tool insert (Figure 1b) and a wiper geometry tool insert (Figure 1c). The Sandvik make of conventional (DCMT11T304-PF) and wiper geometry (DCMX11T304-WF) tool inserts were used to machine AISI 1045 steel [36]. The rake angle for the conventional and wiper geometry tool inserts was 6° and 18°, respectively. However, both inserts had the same cutting-edge angle (55°), clearance angle (7°) and nose radius (0.4 mm). In the processing of the material during turning, the nose radius and feed rate played a pivotal role. Conventional round-nose tool inserts limited productivity. The main reason for this was the limitation of the upper feed value. The possible solution to this problem was to use a large nose radius, which could enhance the forces value along with the chatter. This could either improve productivity or surface quality but not both. With the introduction of wiper geometry in tool inserts, the nose with a large radius of curvature increased productivity with a high feed value. This would increase the surface quality. Feed force (F_f), cutting force

(F_c) and Radial force (Fr) were observed using a Kistler make of dynamometer (Model 5070, (Liechtenstein, Switzerland). The resulting force (R) could be calculated from the formula:

$$R = \sqrt{F_r^2 + F_f^2 + F_c^2}$$

F_r, F_f, F_c and R were computed [38] in Newtons (N). The MRR could be computed using Equation (1).

$$\text{MRR} = 1000\ V_c\ f\ a_p \quad (1)$$

where,

V_c = Surface speed (m/min)
f = Feed rate (mm/rev)
a_p = Depth of cut (mm)
MRR was measured in (mm^3/min)

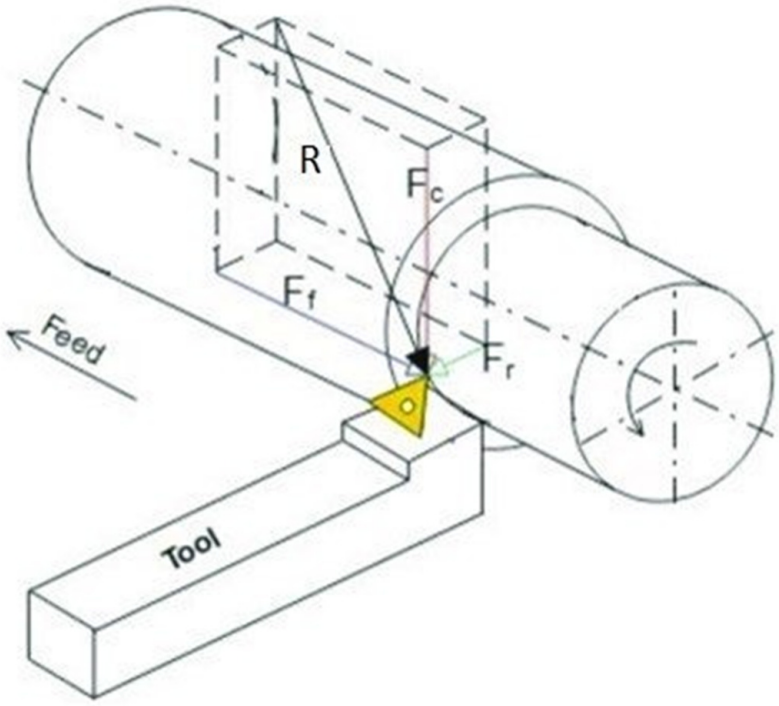

Figure 2. Distribution of forces in turning operation [38].

As reported in [37], the average roughness values measured from the peak and valleys are known as the arithmetic average of the surface roughness (Ra). The value of Ra was measured using the Tesa (Rugosurf 90-G) make (Bugnon, Switzerland) surface roughness tester [37]. The Ra value was measured perpendicular to the axis of cutting. The surface was cleaned with acetone before it was measured, and an average of three readings were selected in the present work for analysis purposes [39,40]. The process flow in the current research is represented in Figure 3.

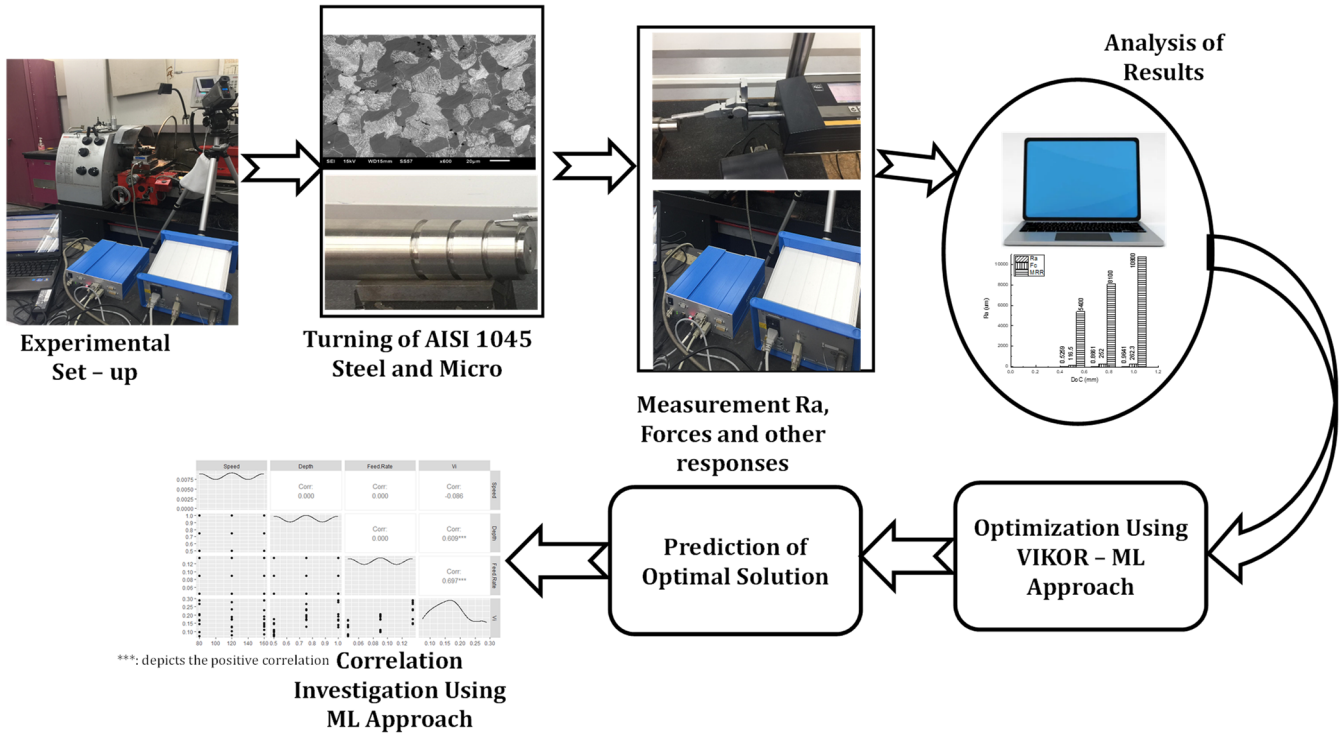

Figure 3. Process flow in the current research.

3. Results and Discussion

The experimental plan of all three input parameters and the corresponding values of R_a, F_r, F_f, F_c, R, Temp and MRR are represented in Figure 4 [37]. The experiments were conducted considering the concept of randomness, repeatability and blocking. It was evident from the responses that out of seven, six (R_a, F_r, F_f, F_c, R, Temp) were of the lower-the-better type, while one (MRR) was a larger-the-best type quality attribute. This made the present problem a Multi-Criteria Decision Making (MCDM) problem [40,41]. Thus, to solve this, the MCDM approach of VIKOR-ML was adopted.

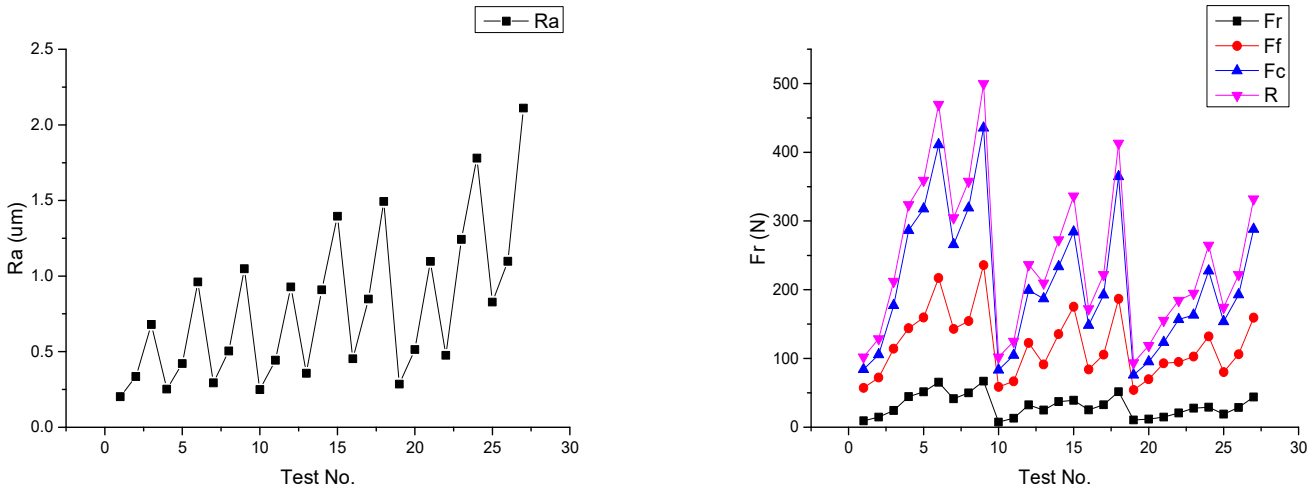

Figure 4. *Cont.*

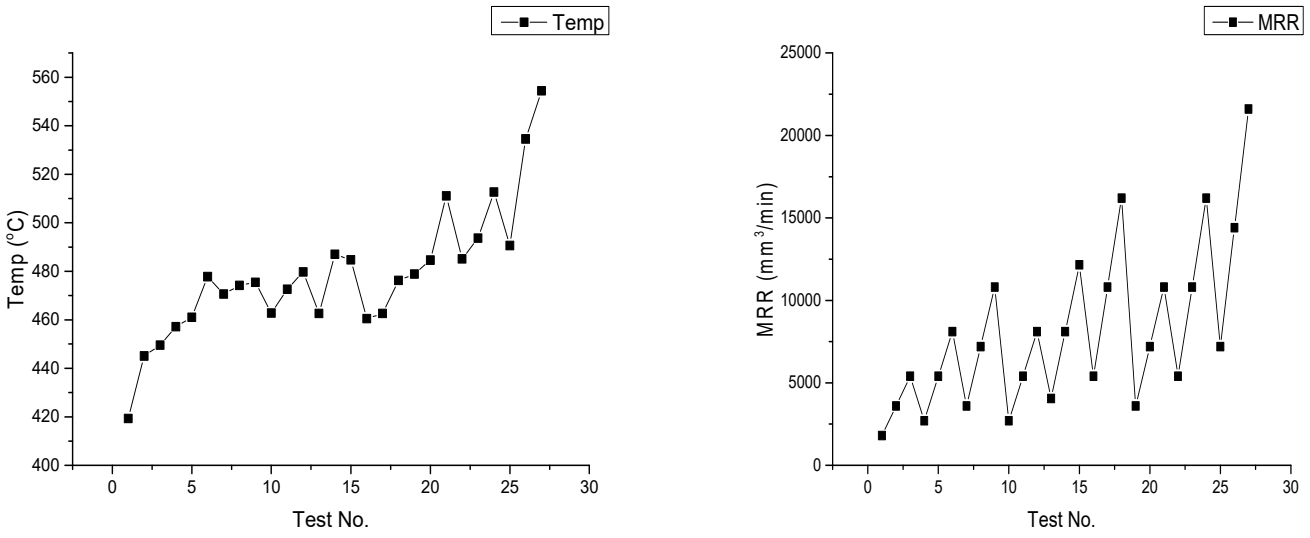

(**c**) (**d**)

Figure 4. Experimental results of 27 experimental tests for (**a**) R_a (**b**) F_r, F_f, F_c and R (**c**) Temp (**d**) MRR.

3.1. Statistical Analysis of Response Variables

Table 2 presents a statistical analysis of the response variables (namely R_a, F_r, F_f, F_c, R, Temp and MRR). From the analysis of R_a, it is clear that *f* had the maximum influence (56.84%) for investigating Ra, preceded by V_c (18.94%) and a_p (14.47%). A high F-value showed the larger contribution of the control factors. The *p*-values in the analysis were the probability value, and for a good model, these were less than 0.05. The interaction of V_c and a_p; a_p and *f*; V_c and f presented *p*-values less than 0.05, which depicted the significant influence of these interactions on the computation of R_a. The value of R^2 predicted the future outcomes of the present model. In the present work, the value of R^2 was 99.09, and Adjusted-was 97.05, which depicted a close agreement with each other.

Table 2. Statistical analysis and ANOVA for various responses.

Source	DF	R_a			F_r			F_f			F_c		
		pcp *	F *	*p* *	pcp	F	*p*	pcp	F	*p*	pcp	F	*p*
V_c	2	18.9	83.39	0	20.4	55.96	0	15.3	97.48	0	18.38	107.7	0
a_p	2	14.4	63.72	0	45.7	125.15	0	35.7	226.92	0	44.58	261.3	0
f	2	56.8	250.2	0	21	57.53	0	38.3	243.12	0	25.6	150.1	0
V_c * a_p	4	3.33	7.32	0.009	8.09	11.08	0.002	5.94	18.84	0	6.88	20.17	0
V_c * *f*	4	2.8	6.16	0.014	1.2	1.63	0.257	1.62	5.14	0.024	1.14	3.33	0.069
a_p * *f*	4	2.71	5.96	0.016	2.12	2.9	0.093	2.35	7.46	0.008	2.74	8.04	0.007
Residual Error	8	0.91	R^2 = 99.09	R^2 (adj) = 97.05	**1.46**	R^2 = 98.54	R^2 (adj) = 95.25	**0.63**	R^2 = 99.37	R^2 (adj) = 99.95	0.68	R^2 = 99.32	R^2 (adj) = 97.78
Total	26	100			100			100			100		

Source	DF	R			Temp			MRR		
		pcp	F	*p*	pcp	F	*p*	pcp	F	*p*
V_c	2	17.9	133.9	0	53.2	42.85	0	21.4	324	0
a_p	2	42.7	320.1	0	11.2	9.07	0.009	21.4	324	0
f	2	28.1	210.8	0	15.9	12.85	0.003	48.1	729	0
V_c * a_p	4	6.75	25.25	0	11.7	4.71	0.03	1.58	12	0.002
V_c * *f*	4	1.2	4.51	0.034	2.81	1.13	0.407	3.56	27	0
a_p * *f*	4	2.63	9.85	0.004	0.11	0.05	0.995	3.56	27	0
Residual Error	8	**0.54**	R^2 = 99.47	R^2 (adj) = 98.26	4.96	R^2 = 95.03	R^2 (adj) = 83.86	0.26	R^2 = 99.74	R^2 (adj) = 99.14
Total	26	100			100			100		

* pcp: Percentage Contribution; * F: F-value; * *p*: *p*-value.

The ANOVA of F_r showed that a_p had a maximum contribution (45.7%), followed by *f* (21%) and V_c (20.4%). The interaction between V_c and a_p played a significant role due to the *p*-value being less than 0.05. Similarly, CS, a_p and *f* had *p*-values less than 0.05 in the case of F_r. The summary of F_f depicted that all the input parameters and respective interactions had a significant influence on the investigations of F_f.

The feed value had a maximum influence (38.3%), followed by a_p (35.7%) and V_c (15.3%). The statistical summary of F_c represented that a_p (44.57%) had a maximum influence on the investigation of Fc while turning AISI 1045 steel using wiper tool inserts, followed by f (25.60%) and V_c (18.37%). The summary suggested that the V_c, a_p, *f*, interaction plots of V_c and *f*, a_p and *f* played an influential effect on the Fc, as evident from the *p*-values. Similar trends were depicted from the F-values. The value of R^2 (99.32%) was in close agreement with the adjusted R^2 (97.78%). R^2 presented the future outcomes from the model due to significant and non-significant terms; however, adjusted-R^2 provided the predictions of future outcomes due to significant terms only. The statistical summary of the reaction ®showed that a_p (42.7%) had a maximum influence on the computation of a response during the turning of AISI 1045 steel using wiper tool inserts, followed by *f* (28.10%) and V_c (17.9%). The summary suggests that V_c, a_p, *f*, the interaction plots of V_c and f, a_p and *f*, V_c and a_p played an influential effect on R, as evident from the *p*-values.

It was evident from the ANOVA that V_c (53.2%) had a maximum influence that was preceded by *f* (15.9%) and a_p (11.2%) for the calculation of temperature during the processing of AISI 1045 steel by wiper geometry. The interaction of CS and a_p also played a significant role in the temperature, with a *p*-value of 0.03, which was less than 0.05. The analysis of MRR revealed that *p*-values for all the parameters and interactions were less than 0.05. Therefore, every parameter and interaction played an important role in the calculation of MRR. From the pcp values it is clear that f had the maximum contribution (48.18%) for the investigation of MRR, preceded by V_c (21.41%) and a_p (21.41%). The values of R^2 and adjusted R^2 for all the responses (namely R_a, F_r, F_f, F_c, R, Temp and MRR) had close compliance with each other.

3.2. Variation in Response Variables with Respect to Machining Variables

The variation in the performance measures with respect to the input process variable is discussed in this section.

It is evident from Figure 5a that with the amplification in the V_c value, the value of the force (F_r, F_f, F_c and R) decreased. This was due to the fact that with the increase in the V_c value from 80 m/min to 160 m/min, the thermal softening of AISI 1045 steel increased due to the value of the force, which decreased gradually. The main fact of this decrement in the Fc with the increase in V_c was the reduction in shear strength as the temperature increased with speed [42]. Another reason for the decrease in Fc might be the tool–chip interface contact area. The contact area was controlled up to a certain length; thus, real contact became smaller than natural contact, and hence Fc was found to be decreased [43]. Figure 5b depicts the variation in the force with respect to a_p, which clarifies that, with the amplification in a_p values, the value of the force was also amplified. This was due to the fact that, with a high value of a_p, more material had to be removed in a single cut at the same V_c and *f*. Therefore, the chances of build-up edges were increased, with the need for large forces to overcome them. Figure 5c represents the variation in the forces with respect to the feed value, and it is clear from Figure 5c that with the increase in the feed value, the value of the force was found to be increased. The probable reason for these enhancements might be that with the increase in the feed value, more material was removed per unit of time. When *f* increased, the relative motion between the workpiece and the tool became faster, leading to higher friction forces. These increased the feed forces and put additional stress on the cutting tool, machine components, and fixtures.

Figure 5d depicts the variation in R_a with the input parameters while machining AISI 1045 steel. The value of R_a was enhanced from 0.5218 µm to 1.048 µm with the increase in the V_c value from 80 to 160 m/min. The value of R_a increased from 0.5218 µm to 0.7663 µm

after varying the V_c value from 80 m/min to 120 m/min. The value of Ra was further enhanced from 0.7663 µm to 1.048 µm with an increase in V_c from 120 to 160 m/min. The main reason for this increment was the material characteristics, which were reactive with the carbide tool inserts [44]. During the machining process, the material was removed in the form of chips. These chips were stuck with the cutting tool and made the surface quality poor. With the increase in V_c, more chips were exposed to the surface, and surface roughness increased. It was found that the value of R_a ameliorated from 0.525 µm to 0.964 µm with an increase in the a_p value from 0.5 mm to 1 mm. The main reason for the increase in the R_a value with a_p was the increase in the depth of the tool. Due to this, more material was plowed from the workpiece in the form of craters that increased the Ra. It was found that the value of Ra increased from 0.3773 µm to 0.7017 µm with the amplification in the f value from 0.045 mm/rev to 0.09 mm/rev. Further, an increase in the *f* value from 0.09 mm/rev to 0.135 mm/rev, and the value of R_a was enhanced from 0.701 µm to 1.277 µm. This enhancement in roughness value was due to more material being extracted from the workpiece with each revolution. Thus, large craters were removed, which made the surface poorer.

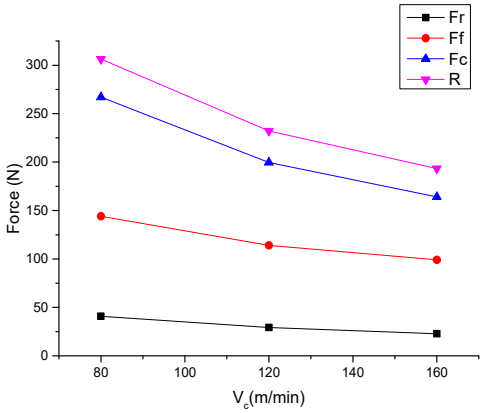

(**a**) Forces versus Vc

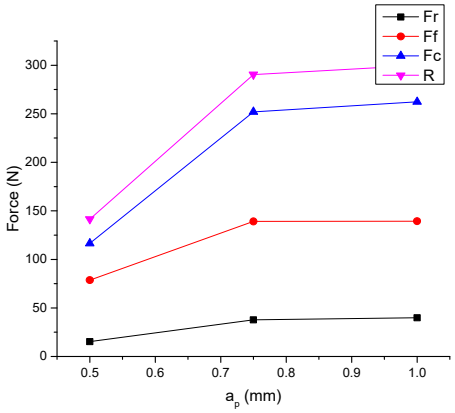

(**b**) Forces versus ap

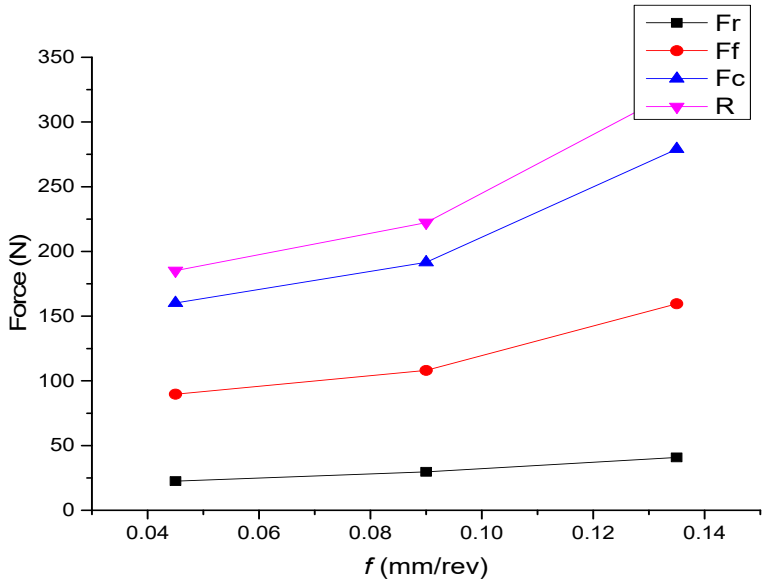

(**c**) Forces versus f

Figure 5. *Cont.*

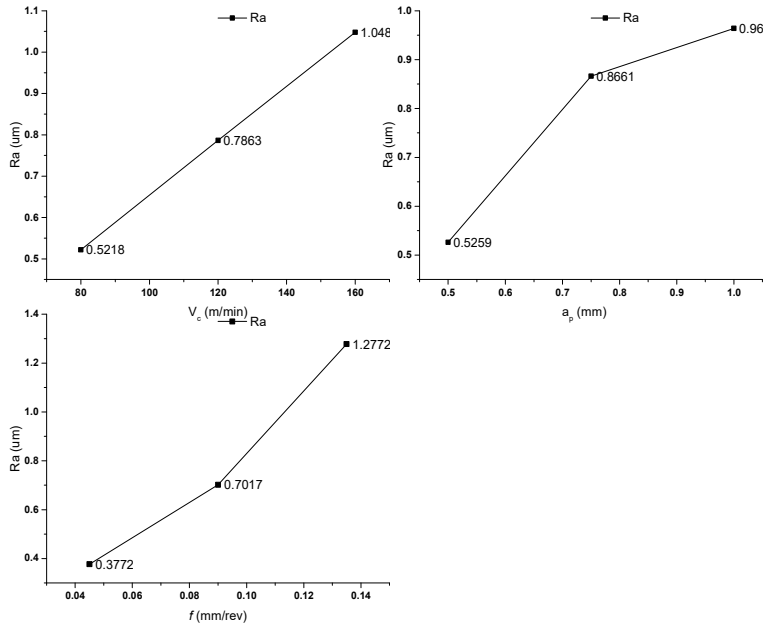

(**d**) Variation in Ra with respect to input parameters

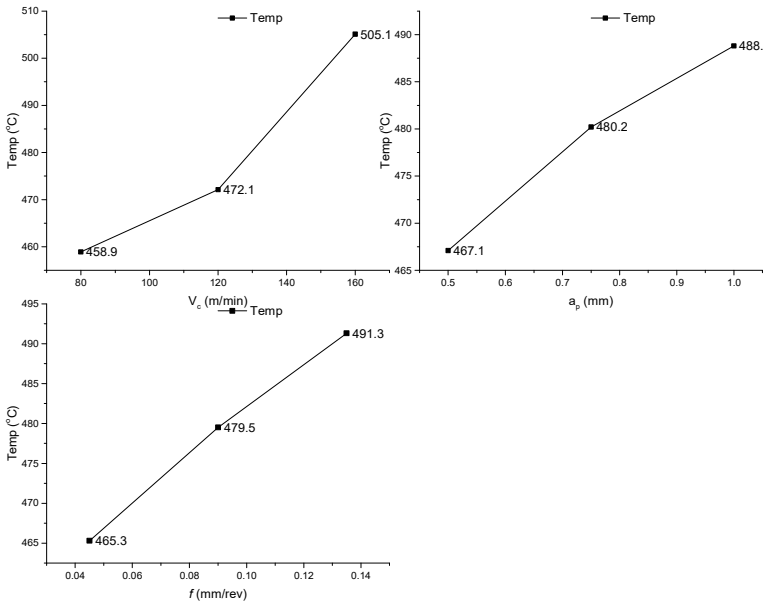

(**e**) Variation in Temp with respect to input parameters

Figure 5. *Cont*.

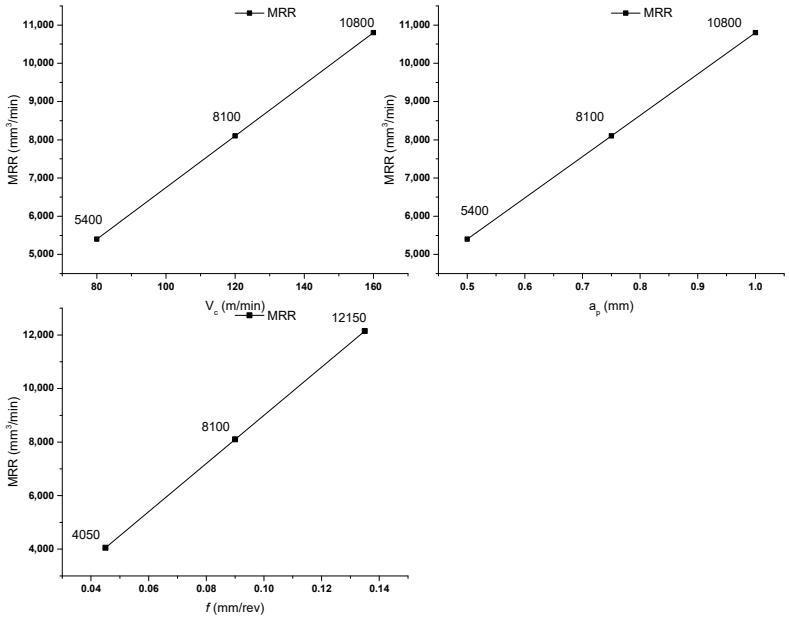

(**f**) Variation in MRR with respect to input parameters

Figure 5. Variation in performance measures with respect to process parameters (**a**) Forces versus Vc (**b**) Forces versus a_p (**c**) Forces versus f (**d**) Variation in Ra with respect to input parameters (**e**) Variation in temperature with respect to input parameters (**f**) Variation in MRR with respect to input parameters.

Figure 5e presents the variation in temperature with the change in machining variables. It is clear from Figure that with the increase in V_c, f and a_p, the temperature also increased. Machining takes place due to plastic deformation, and during deformation, most of the energy is converted into heat. With the increase in a_p and V_c, larger amounts of heat were generated, which increased the temperature. The increase in the feed value increased the friction between the tool and chip and increased the cutting temperature. Figure 5f depicts the variation in MRR with the input parameters. Figure 5a shows that with the increase in V_c from 80 m/min to 160 m/min, the MRR increased from 5400 mm^3/min to 10,800 mm^3/min. The increase in MRR was due to more material coming into contact with the tool at the same time as an increase in V_c. The value of MRR increased from 5400 mm^3/min to 8100 mm^3/min with the amelioration of a_p from 0.5 mm to 0.75 mm. A further increase in the a_p value took place from 0.75 mm to 1 mm, and MRR was observed to increase from 8100 mm^3/min to 10,800 mm^3/min. The increase in MRR was due to an increase in more material depth with the increase in the a_p value. With the increase in the f value, the chip load per revolution was enhanced, and MRR was found to be increased. Due to the increase in the chip load per revolution, the MRR value increased from 4050 mm^3/min to 12,150 mm^3/min with the increase in f from 0.045 mm/rev to 0.135 mm/rev.

4. Implementation of VIKOR-ML Approach

4.1. VIKOR Approach

The VIKOR method is a statistical method that can solve the problems associated with multiple responses having conflicting natures (like the combination of the smaller the better and higher the best type quality attributes for a single problem). A Serbian researcher Sarafim Opricoveic developed this method in 1979 to solve MCDM problems, and in 1980, the researcher applied it for the first time. In 1990, it was named VIKOR, which is extracted from a Serbian word [45], which means Multi-Criteria Optimization and Compromised Solutions. This method was effectively used to find out the best solution where the process involved either two or more than two response variables. In the present

research, seven output responses (i.e., R_a, F_f, F_r, F_c, R, Temp and MRR) were involved, in which two responses (R_a, F_f, F_r, F_c, R and Temp) were of the lower the better type while MRR had a higher the better type quality attribute, which made it a combination of both types of responses (those are conflicting in nature) [46].

Few responses have values in thousands, while others have values in hundreds or in decimals. Thus, it became essential to normalize all the responses and categorize all the response variables between zero and one. The standard process was adopted for the normalization [47]. The decision matrix was formed according to Equation (2).

$$H = \begin{bmatrix} H_{11} & H_{12} & . & . & H_{1n} \\ H_{21} & H_{22} & . & . & H_{2n} \\ . & . & . & . & . \\ . & . & . & . & . \\ H_{m1} & H_{m2} & . & . & H_{mn} \end{bmatrix} \quad (2)$$

Here, n are the responses and i = 1, 2, ... , m are the input variables.

Once the decision matrix was formed, the normalization of the data was processed as per Equation (2). The response variables had different units and different orders; thus, after the normalization all the responses were transformed into a dimensionless number between 0 and 1. The normalized values of all the performance measures were evaluated and are depicted in Table 3. All the normalized values were summed up, and the performance index was calculated and described here as the VIKOR index (V_i). A large value of V_i depicted the best optimal setting for the compromised results, where all three-response variables could be compromised.

$$\overline{H}_{ij} = \frac{H_{ij}}{\sqrt{\sum_{i=1}^{n} H_{ij}^2}} \quad (3)$$

Table 3. Weighted normalization of responses and the calculation of V_i.

Test No.	W Normalized MRR	W Normalized Ra	Normalized F_c	Normalized F_r	Normalized F_f	Normalized R	Normalized Temp	Pi
1	0.0052	0.0059	0.0097	0.0069	0.0120	0.0103	0.0236	0.0735
2	0.0103	0.0097	0.0122	0.0113	0.0152	0.0129	0.0250	0.0967
3	0.0155	0.0198	0.0205	0.0186	0.0240	0.0213	0.0253	0.1450
4	0.0077	0.0073	0.0332	0.0342	0.0302	0.0325	0.0257	0.1709
5	0.0155	0.0122	0.0368	0.0395	0.0335	0.0361	0.0259	0.1996
6	0.0232	0.0279	0.0476	0.0503	0.0456	0.0472	0.0269	0.2687
7	0.0103	0.0085	0.0308	0.0318	0.0300	0.0306	0.0264	0.1685
8	0.0206	0.0146	0.0370	0.0383	0.0324	0.0360	0.0266	0.2055
9	0.0310	0.0304	0.0504	0.0513	0.0495	0.0502	0.0267	0.2896
10	0.0077	0.0072	0.0096	0.0057	0.0123	0.0103	0.0260	0.0789
11	0.0155	0.0129	0.0121	0.0099	0.0140	0.0126	0.0266	0.1035
12	0.0232	0.0270	0.0231	0.0249	0.0258	0.0238	0.0270	0.1747
13	0.0116	0.0104	0.0217	0.0191	0.0192	0.0211	0.0260	0.1290
14	0.0232	0.0264	0.0270	0.0286	0.0284	0.0274	0.0274	0.1884
15	0.0348	0.0405	0.0329	0.0300	0.0368	0.0338	0.0272	0.2362
16	0.0155	0.0132	0.0172	0.0193	0.0176	0.0173	0.0259	0.1260
17	0.0310	0.0246	0.0223	0.0250	0.0222	0.0223	0.0260	0.1734
18	0.0464	0.0434	0.0423	0.0396	0.0392	0.0415	0.0268	0.2792
19	0.0103	0.0083	0.0088	0.0080	0.0113	0.0094	0.0269	0.0831
20	0.0206	0.0149	0.0110	0.0090	0.0146	0.0119	0.0272	0.1094
21	0.0310	0.0319	0.0143	0.0113	0.0195	0.0156	0.0287	0.1523
22	0.0155	0.0138	0.0181	0.0159	0.0199	0.0185	0.0273	0.1290

Table 3. *Cont.*

Test No.	W Normalized MRR	W Normalized Ra	Normalized F_c	Normalized F_r	Normalized F_f	Normalized R	Normalized Temp	Pi
23	0.0310	0.0361	0.0189	0.0212	0.0216	0.0196	0.0277	0.1761
24	0.0464	0.0517	0.0264	0.0223	0.0277	0.0266	0.0288	0.2300
25	0.0206	0.0240	0.0178	0.0146	0.0168	0.0175	0.0276	0.1391
26	0.0413	0.0319	0.0223	0.0220	0.0223	0.0223	0.0300	0.1922
27	0.0619	0.0613	0.0334	0.0337	0.0335	0.0334	0.0312	0.2883

Table 3 presents the V_i values and the maximum value of V_i (0.2883) was found corresponding to experimental run number 27. Corresponding to experiment number 27 the values of R_a, F_r, F_f, F_c, R, temp and MRR were 2.111 µm, 43.85 N, 159.33 N, 288.13 N, 332,16 N, 554.4 °C and 21,600 mm^3/min, respectively.

4.2. Machine Learning Approach

The optimization was conducted using the empirical modeling and machine learning approach. The objectives in the present work were larger the better the type (MRR) and lower the better (R_a, F_r, F_f, F_c, R and temp) [48,49]. 'V_i' is the objective function in the current work. V_i was the combined effect of R_a, F_r, F_f, F_c, R, temp and MRR; therefore, it became larger the better type of quality characteristic. The larger the value of V_i, the better the compromised result of R_a, F_r, F_f, F_c, R, temp and MRR corresponding to the parametric setting. To optimize the value of V_i, the machine learning approach was implemented. In this approach, the first step included the extraction of data in the Excel format and then provided the local namespace. In the second step, Pandas and NumPy were used for the analysis of data. The prerequisite for Pandas was already explained in the previous research [49–52], which included the data frame and series. Further, the correlation was investigated between the input variables (V_c, f and a_p) and the collective output parameter (V_i).

This correlation was set up by the visualization and evaluation of datasets. The data in V_i Table (Table 3) were divided into two portions: one portion was used for the training purpose (80% data), and the other portion was used for testing (20% data). Figure 6 shows the correlation mapping of the process parameters with respect to V_i. It is clear from Figure 6 that there was a correlation between V_i and V_c and V_i and a_p, V_i and f. From the color mapping, the darkest color was observed in the case of V_i and f, while it faded away in the case of V_i and a_p. The values of correlation between the process parameters and V_i can be observed in Figure 7. The maximum value of the correlation was 0.697 (in the case of V_i and f). Further, its value decreased to 0.609 (V_i and a_p) and −0.086 (V_i and V_c). Therefore, the correlation mapping and correlation plot verified the results.

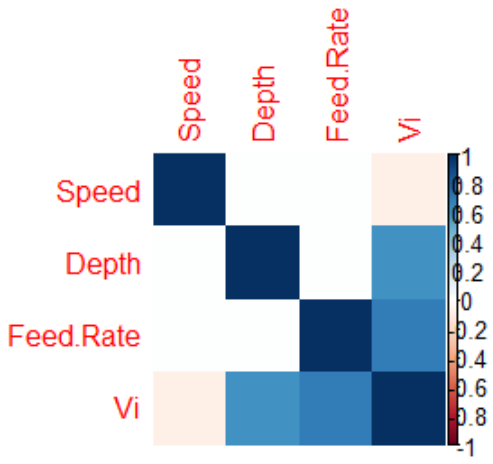

Figure 6. Correlation mapping between process parameters and V_i.

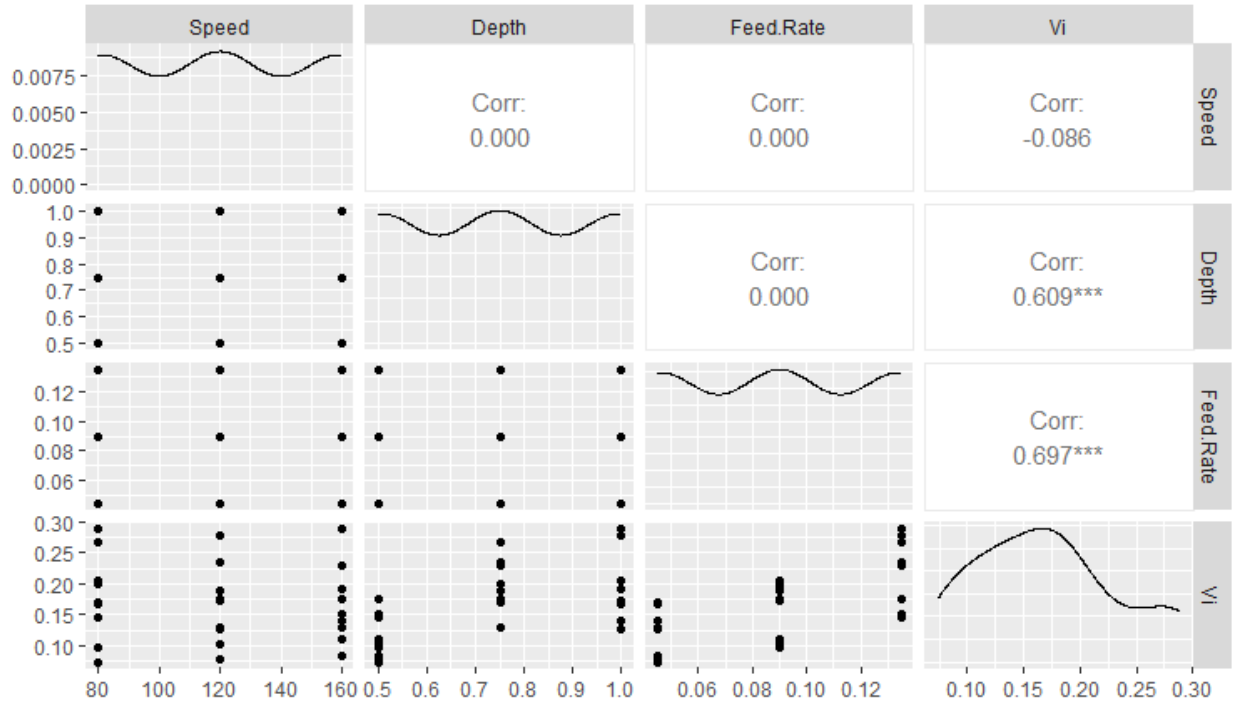

***: depicts the positive correlation.

Figure 7. Correlation plot between process parameters and V_i.

5. Conclusions

In the current work, a previously reported experimental investigation into the machining responses of AISI 1045 steel using wiper geometry tool inserts on a tuning operation was further extended. The performance of the process was evaluated in terms of R_a, F_r, F_f, F_c, R, temperature and MRR while varying V_c, a_p and f. The collective output of the process was investigated using the integrated VIKOR Machine Learning Approach. The outcomes from the present work are as follows:

1. Feed (*f*) had the maximum influence (56.84%) on R_a while turning AISI 1045 steel, followed by V_c (18.94%) and a_p (14.47%). The interactions of V_c and a_p, V_c and *f* and a_p and *f* had a significant influence on the investigation of R_a due to a *p*-value less than 0.05.
2. For the investigation of F_r, a_p had the maximum influence (45.7%), followed by f (21%) and V_c (20.4%). However, in the investigation of F_f, f played a pivotal role (38.3%), preceded by a_p (35.7%) and V_c (15.3%). In the calculation of F_c, the a_p contribution was 44.57%, followed by f (25.60%) and V_c (18.37%). Due to a *p*-value less than 0.05 for the interactions of V_c and a_p and *f* and a_p, a major contribution to the calculation of F_c was observed during the turning of AISI 1045 steel by the carbide tool (wiper edge geometry). However, in the investigation of Ff, f played a pivotal role. As 'R' was the combination of all the forces; thus, all the input parameters and their interactions had an influential effect on the investigation of the reaction (R).
3. For the investigation of MRR, *f* had the major role (48.18%), followed by a_p and V_c with 21.41% each. All the interactions (V_c and a_p; V_c and f; a_p and *f*) also had a major contribution to MRR. The values of R^2 and Adj-R^2 for all the performance measures were greater than 95%, which signified the outperformance of the present work for future outcomes.
4. The VIKOR-based performance index (V_i) suggests the best optimal setting, which was V_c: 160 m/min; a_p: 1 mm; *f*: 0.135 mm/rev. Corresponding to this optimal setting, the V_i value was maximum (0.2883). The value of performance measured R_a, F_r, F_f, F_c,

R, temperature and MRR, which were 2.111 µm, 43.85 N, 159.33 N, 288.13 N, 332,16 N, 554.4 °C and 21,600 mm^3/min, respectively, corresponding to this setting.

5. The ML approach investigated the correlation between the input process variables and V_i, by which a strong correlation could be observed between V_i and f (0.697), followed by V_i and a_p (0.609) and V_i and V_c (−0.086). The proposed approach of V_i-ML could be effectively used for the investigation of parametric optimization and correlation mapping.

In the near future, the proposed approach could be used for the investigation of other responses like other roughness parameters, surface integrity, etc. The other processes, like milling, drilling, welding and other non-traditional processes, could be analyzed using the Vi-ML approach.

Author Contributions: A.T.A., N.S. and A.E.: investigation, conceptualization, methodology, data curation, validation, visualization; M.S.S., M.M.E.R. and R.C.S.: investigation, writing—original draft, writing, conceptualization, supervision, project administration: Review and editing; A.T.A.: funding acquisition. All authors have read and agreed to the published version of the manuscript.

Funding: Grant Number (IFKSUOR3-040-2).

Data Availability Statement: Not applicable.

Acknowledgments: The authors extend their appreciation to the Deputyship for Research and Innovation, Ministry of Education in Saudi Arabia for funding this research work through the project no. (IFKSUOR3–040-2).

Conflicts of Interest: The authors declare that they have no known competing financial interests or personal relationships that could have appeared to influence the work reported in this paper.

References

1. Ruibin, X.; Wu, H. Study on Cutting Mechanism of Ti6Al4V in Ultra-Precision Machining. *Int. J. Adv. Manuf. Technol.* **2016**, *86*, 1311–1317. [CrossRef]
2. Selvam, M.D.; Senthil, P. Investigation on the Effect of Turning Operation on Surface Roughness of Hardened C45 Carbon Steel. *Aust. J. Mech. Eng.* **2016**, *14*, 131–137. [CrossRef]
3. Sharma, A.K.; Tiwari, A.K.; Dixit, A.R. Effects of Minimum Quantity Lubrication (MQL) in Machining Processes Using Conventional and Nanofluid Based Cutting Fluids: A Comprehensive Review. *J. Clean. Prod.* **2016**, *127*, 1–18. [CrossRef]
4. Leppert, T. Effect of Cooling and Lubrication Conditions on Surface Topography and Turning Process of C45 Steel. *Int. J. Mach. Tools Manuf.* **2011**, *51*, 120–126. [CrossRef]
5. Walker, T. *The MQL Handbook, A Guide to Machining with Minimum Quantity Lubrication*; V1.0.7; 2015; Unist, Inc.: Grand Rapids, MI, USA, 2015.
6. Le Coz, G.; Marinescu, M.; Devillez, A.; Dudzinski, D.; Velnom, L. Measuring Temperature of Rotating Cutting Tools: Application to MQL Drilling and Dry Milling of Aerospace Alloys. *Appl. Therm. Eng.* **2012**, *36*, 434–441. [CrossRef]
7. Hamdan, A.; Sarhan, A.; Hamdi, M. An Optimization Method of the Machining Parameters in High-Speed Machining of Stainless Steel Using Coated Carbide Tool for Best Surface Finish. *Int. J. Adv. Manuf. Technol.* **2012**, *58*, 81–91. [CrossRef]
8. Kurgin, S.; Dasch, J.M.; Simon, D.L.; Barber, G.C.; Zou, Q. Evaluation of the Convective Heat Transfer Coefficient for Minimum Quantity Lubrication (MQL). *Ind. Lubr. Tribol.* **2012**, *64*, 376–386. [CrossRef]
9. Elmunafi, M.H.S.; Kurniawan, D.; Noordin, M.Y. Use of Castor Oil as Cutting Fluid in Machining of Hardened Stainless Steel with Minimum Quantity of Lubricant. *Procedia Cirp* **2015**, *26*, 408–411. [CrossRef]
10. Debnath, S.; Reddy, M.M.; Yi, Q.S. Environmental Friendly Cutting Fluids and Cooling Techniques in Machining: A Review. *J. Clean. Prod.* **2014**, *83*, 33–47. [CrossRef]
11. Rahim, E.A.; Sasahara, H. An Analysis of Surface Integrity When Drilling Inconel 718 Using Palm Oil and Synthetic Ester under MQL Condition. *Mach. Sci. Technol.* **2011**, *15*, 76–90. [CrossRef]
12. Lawal, S.A.; Choudhury, I.A.; Nukman, Y. A Critical Assessment of Lubrication Techniques in Machining Processes: A Case for Minimum Quantity Lubrication Using Vegetable Oil-Based Lubricant. *J. Clean. Prod.* **2013**, *41*, 210–221. [CrossRef]
13. Schwarz, M.; Dado, M.; Hnilica, R.; Veverková, D. Environmental and Health Aspects of Metalworking Fluid Use. *Polish J. Environ. Stud.* **2015**, *24*, 37–45.
14. Islam, M.N.; Anggono, J.M.; Pramanik, A.; Boswell, B. Effect of Cooling Methods on Dimensional Accuracy and Surface Finish of a Turned Titanium Part. *Int. J. Adv. Manuf. Technol.* **2013**, *69*, 2711–2722. [CrossRef]
15. Raynor, P.C.; Kim, S.W.; Bhattacharya, M. Mist Generation from Metalworking Fluids Formulated Using Vegetable Oils. *Ann. Occup. Hyg.* **2005**, *49*, 283–293.

16. Davim, J.P. *Green Manufacturing Processes and Systems*; Springer: Berlin/Heidelberg, Germany, 2013; ISBN 3642337929.
17. Boubekri, N.; Shaikh, V.; Foster, P.R. A Technology Enabler for Green Machining: Minimum Quantity Lubrication (MQL). *J. Manuf. Technol. Manag.* **2010**, *21*, 556–566. [CrossRef]
18. Astakhov, V. Ecological Machining: Near-dry Machining. In *Machining*; Springer: London, UK, 2008. [CrossRef]
19. Selvam, M.D.; Sivaram, N. The Effectiveness of Various Cutting Fluids on the Surface Roughness of AISI 1045 Steel during Turning Operation Using Minimum Quantity Lubrication System. *J. Futur. Eng. Technol.* **2017**, *13*, 36–43.
20. Krishnaraj, V.; Krishna, B.H.; Sheikh-Ahmad, J.Y. An Experimental Study on End Milling of Titanium Alloy (Ti-6Al-4V) under Dry and Minimum Quantity Lubrication Conditions. *Int. J. Mach. Mach. Mater.* **2017**, *19*, 325–342. [CrossRef]
21. Babu, M.N.; Manimaran, G.; Muthukrishnan, N. Experimental Estimation of Minimum Quantity Lubrication in Turning on AISI 410 Stainless Steel. *Int. J. Mach. Mach. Mater.* **2017**, *19*, 522–537. [CrossRef]
22. Chinchanikar, S.; Choudhury, S.K. Comparative Evaluations of Nose Wear Progression and Failure Modes during Hard Turning under Dry and Near-Dry Cutting Conditions. *Int. J. Mach. Mach. Mater.* **2016**, *18*, 466–482. [CrossRef]
23. Boswell, B.; Islam, M.N. The Challenge of Adopting Minimal Quantities of Lubrication for End Milling Aluminium. In Proceedings of the IAENG Transactions on Engineering Technologies: Special Volume of the World Congress on Engineering, London, UK, 4–6 July 2012; Springer: Berlin/Heidelberg, Germany, 2013; pp. 713–724.
24. Singh, T.; Singh, P.; Dureja, J.S.; Dogra, M.; Singh, H.; Bhatti, M.S. A Review of near Dry Machining/Minimum Quantity Lubrication Machining of Difficult to Machine Alloys. *Int. J. Mach. Mach. Mater.* **2016**, *18*, 213–251. [CrossRef]
25. Nicolo, B. *Quality by Design: Taguchi Techniques for Industrial Experimentation*; Prentice Hall: Hoboken, NJ, USA, 1995; ISBN 0-13-186362-2.
26. Sivaiah, P.; Chakradhar, D. Performance Improvement of Cryogenic Turning Process during Machining of 17-4 PH Stainless Steel Using Multi Objective Optimization Techniques. *Meas. J. Int. Meas. Confed.* **2019**, *136*, 326–336. [CrossRef]
27. Manikandan, N.; Kumanan, S.; Sathiyanarayanan, C. Optimisation of Electrochemical Drilling Process Using Taguchi Method and Regression Analysis. *Int. J. Mach. Mach. Mater.* **2017**, *19*, 136–159. [CrossRef]
28. Goel, B.; Singh, S.; Sarepaka, R.G. V Optimisation of Machining Parameters for Single Point Diamond Turning of Chromium Zirconium Copper Alloy C18150 Using Taguchi and Grey Relational Analysis. *Int. J. Mach. Mach. Mater.* **2017**, *19*, 95–109. [CrossRef]
29. Bajić, D.; Lela, B.; Živković, D. Modeling of Machined Surface Roughness and Optimization of Cutting Parameters in Face Milling. *Metalurgija* **2008**, *47*, 331–334.
30. Yang, J.L.; Chen, J.C. A Systematic Approach for Identifying Optimum Surface Roughness Performance in End-Milling Operations. *J. Ind. Technol.* **2001**, *17*, 1–8.
31. Caldeirani Filho, J.; Diniz, A.E. Influence of Cutting Conditions on Tool Life, Tool Wear and Surface Finish in the Face Milling Process. *J. Brazilian Soc. Mech. Sci.* **2002**, *24*, 10–14. [CrossRef]
32. Tsao, C.C. Grey–Taguchi Method to Optimize the Milling Parameters of Aluminum Alloy. *Int. J. Adv. Manuf. Technol.* **2009**, *40*, 41–48. [CrossRef]
33. Abbas, A.T.; Gupta, M.K.; Soliman, M.S.; Mia, M.; Hegab, H.; Luqman, M.; Pimenov, D.Y. Sustainability Assessment Associated with Surface Roughness and Power Consumption Characteristics in Nanofluid MQL-Assisted Turning of AISI 1045 Steel. *Int. J. Adv. Manuf. Technol.* **2019**, *105*, 1311–1327. [CrossRef]
34. Abbas, A.T.; Al-Abduljabbar, A.A.; Alnaser, I.A.; Aly, M.F.; Abdelgaliel, I.H.; Elkaseer, A. A Closer Look at Precision Hard Turning of AISI4340: Multi-Objective Optimization for Simultaneous Low Surface Roughness and High Productivity. *Materials* **2022**, *15*, 2106. [CrossRef]
35. Abbas, A.T.; Al-Abduljabbar, A.A.; El Rayes, M.M.; Benyahia, F.; Abdelgaliel, I.H.; Elkaseer, A. Multi-Objective Optimization of Performance Indicators in Turning of AISI 1045 under Dry Cutting Conditions. *Metals* **2023**, *13*, 96. [CrossRef]
36. Abbas, A.T.; El Rayes, M.M.; Al-Abduljabbar, A.A.; Ragab, A.E.; Benyahia, F.; Elkaseer, A. Effects of Tool Edge Geometry and Cutting Conditions on the Performance Indicators in Dry Turning AISI 1045 Steel. *Machines* **2023**, *11*, 397. [CrossRef]
37. Szwajka, K.; Trzepiecinski, T. On the Machinability of Medium Density Fiberboard by Drilling. *BioResources* **2018**, *13*, 8263–8278. [CrossRef]
38. Nur, R.; Yusof, N.M.; Sudin, I.; Nor, F.M.; Kurniawan, D. Determination of Energy Consumption during Turning of Hardened Stainless Steel Using Resultant Cutting Force. *Metals* **2021**, *11*, 565. [CrossRef]
39. Szwajka, K.; Zielińska-Szwajka, J.; Trzepiecinski, T. Experimental Study on Drilling MDF with Tools Coated with TiAlN and ZrN. *Materials* **2019**, *12*, 386. [CrossRef]
40. Sharma, N.; Gupta, R.D.; Khanna, R.; Sharma, R.C.; Sharma, Y.K. Machining of Ti-6Al-4V Biomedical Alloy by WEDM: Investigation and Optimization of MRR and Rz Using Grey-Harmony Search. *World J. Eng.* **2021**, *20*, 221–234. [CrossRef]
41. Abbas, A.T.; Sharma, N.; Alsuhaibani, Z.A.; Sharma, V.S.; Soliman, M.S.; Sharma, R.C. Processing of Al/SiC/Gr Hybrid Composite on EDM by Different Electrode Materials Using RSM-COPRAS Approach. *Metals* **2023**, *13*, 1125. [CrossRef]
42. Demir, H.; Gündüz, S. The Effects of Aging on Machinability of 6061 Aluminium Alloy. *Mater. Des.* **2009**, *30*, 1480–1483. [CrossRef]
43. Shaw, M.C.; Cookson, J.O. *Metal Cutting Principles*; Oxford University Press: New York, NY, USA, 2005; Volume 2.
44. Hosseini, A.; Kishawy, H.A. Cutting Tool Materials and Tool Wear. In *Machining of Titanium Alloys*; Springer: Berlin/Heidelberg, Germany, 2014; pp. 31–56. [CrossRef]
45. Opricovic, S.; Tzeng, G.-H. Compromise Solution by MCDM Methods: A Comparative Analysis of VIKOR and TOPSIS. *Eur. J. Oper. Res.* **2004**, *156*, 445–455. [CrossRef]

46. Gul, M.; Celik, E.; Aydin, N.; Gumus, A.T.; Guneri, A.F. A State of the Art Literature Review of VIKOR and Its Fuzzy Extensions on Applications. *Appl. Soft Comput.* **2016**, *46*, 60–89. [CrossRef]
47. Khan, A.; Maity, K.P. A novel MCDM approach for simultaneous optimization of some correlated machining parameters in turning of CP-titanium grade 2. *Int. J. Eng. Res. Africa* **2016**, *22*, 94–111. [CrossRef]
48. Sharma, N.; Ahuja, N.; Goyal, R.; Rohilla, V. Parametric optimization of EDD using RSM-Grey-TLBO-based MCDM approach for commercially pure titanium. *Grey Sys.: Theory Appl.* **2020**, *10*, 231–245. [CrossRef]
49. Shahali, H.; Yazdi, M.R.S.; Mohammadi, A.; Iimanian, E. Optimization of Surface Roughness and Thickness of White Layer in Wire Electrical Discharge Machining of DIN 1.4542 Stainless Steel Using Micro-Genetic Algorithm and Signal to Noise Ratio Techniques. *Proc. Inst. Mech. Eng. Part B J. Eng. Manuf.* **2012**, *226*, 803–812. [CrossRef]
50. Vendan, S.A.; Kamal, R.; Karan, A.; Gao, L.; Niu, X.; Garg, A. *Welding and Cutting Case Studies with Supervised Machine Learning*; Springer: Berlin/Heidelberg, Germany, 2020; Volume 1, ISBN 9811393818.
51. Bisaria, H.; Shandilya, P. Wire Electric Discharge Machining Induced Surface Integrity for Ni55. 95Ti44. 05 Shape Memory Alloy. *Proc. Inst. Mech. Eng. Part E J. Process Mech. Eng.* **2021**, *235*, 178–185. [CrossRef]
52. Kumar, A.; Sharma, R.; Gupta, A.K. Experimental Investigation of WEDM Process through Integrated Desirability and Machine Learning Technique on Implant Material. *J. Mech. Behav. Mater.* **2021**, *30*, 38–48. [CrossRef]